

# Photodegradation of Reactive Black BL-G by Anatase TiO<sub>2</sub>-Graphene Nanocomposites

K. REN<sup>1, a</sup>, S. G. PAN<sup>2, b,\*</sup> and Y. S. FU<sup>3, c,\*</sup>

<sup>1</sup>Zhoukou Normal University, Zhoukou, Henan, 466001, China

<sup>2</sup>Changzhou Vocational Institute of Light Industry, Changzhou, Jiangsu, 213164, China

<sup>3</sup>Nanjing University of Science and Technology, Nanjing, Jiangsu, 210094, China

<sup>a</sup>515213581@qq.com, <sup>b</sup>panshugang2010@163.com, <sup>c</sup>14336069@qq.com

\*Corresponding author

**Keywords:** Photodegradation, Anatase TiO<sub>2</sub> Nanoparticles, Graphene, Heat treatment.

**Abstract.** Anatase TiO<sub>2</sub>-graphene (ATG) nanocomposites were prepared via a facile one-step solvothermal method. The samples were characterized by X-ray diffraction (XRD), Fourier transform infrared (FT-IR) spectroscopy, Raman spectra and transmission electron microscopy (TEM). During the solvothermal reaction, anatase TiO<sub>2</sub> nanoparticles with diameters ranging from 5 to 10 nm were deposited on the carbon sheets, and the deoxygenation of graphite oxide (GO) was achieved at the same time. Compared with the mere anatase TiO<sub>2</sub> nanoparticles, the combination of anatase TiO<sub>2</sub> nanoparticles and graphene produced a significant effect on its photocatalytic activity evaluated by the degradation test of Reactive Black BL-G (RB BL-G) under UV irradiation. Our studies also determined the relative influences of the mass ratio of TiO<sub>2</sub>/GO and heat treatment temperature on the photocatalytic activities.

## Introduction

Over the past decades, TiO<sub>2</sub> has been received widely interest due to its photocatalytic properties, high photostability, and relative nontoxicity.<sup>[1-5]</sup> For TiO<sub>2</sub>, there are three naturally occurring polymorphs, anatase, rutile and brookite.<sup>[6]</sup> It is generally accepted that the anatase phase is the most active in photocatalytic application, and the high crystallinity and large surface area are beneficial to improve the photoactivity.<sup>[7, 8]</sup> Among various TiO<sub>2</sub>-based materials, the composites of TiO<sub>2</sub> and carbon (TiO<sub>2</sub>-C) are currently being considered for many applications including their potential use to address the escalating environment problems.<sup>[9]</sup> However, there are still several problems hinder the further applications of the present TiO<sub>2</sub>-C composites, for example, the marked decrease in adsorptivity and a reduction in the amount of UV rays reaching the anatase surface.<sup>[9, 10]</sup> In order to overcome these disadvantages, it is of great significance to explore new carbon substrates and design facile routes to obtain novel TiO<sub>2</sub>-C composites possessing high photocatalytic activity.

Graphene, a one-atom-thick sheet of hexagonally arrayed sp<sup>2</sup>-bonded carbon atoms, has exhibited outstanding mechanical, thermal, electrical, and optical properties and extremely high specific surface area (2600m<sup>2</sup>/g).<sup>[11-13]</sup> In view of the unique structure of graphene, the combination of TiO<sub>2</sub> and graphene is promising to enhance the charge separation and decrease the possibility of recombination of electron-hole pairs in electron-transfer processes, which increase the number of holes participated in the photooxidation process and enhanced the photocatalytic activity.<sup>[14]</sup> Some studies have focused on the application of TiO<sub>2</sub>-graphene composites in Li-ion insertion properties,<sup>[15]</sup> UV-Assisted photoreduction of the graphite oxide (GO),<sup>[16]</sup> and hydrogen evolution from water photo-splitting under UV-vis illumination.<sup>[17]</sup> To the best of our knowledge, few studies on the photodegradation of organic pollutant of anatase TiO<sub>2</sub>-graphene (ATG) have been reported so far. Most recently, P25-graphene photocatalyst was reported to show higher performance than bare P25,<sup>[18]</sup> while the synthesis of high performance and low-cost TiO<sub>2</sub>-graphene composites still need further study. Herein, we describe a facile and controllable solvothermal route to synthesis of ATG nanocomposite possessing much higher photocatalytic activity than pure anatase TiO<sub>2</sub>.

## Experimental

### Preparation

GO was prepared from powdered flake graphite (400 mesh) by a modified Hummers method as described previously<sup>[19, 20]</sup> Nanocomposites with different mass ratios of TiO<sub>2</sub>/GO were synthesized. The typical route, for example, when the mass ratio of TiO<sub>2</sub>/GO was 6:1, is as follows: A 80 mg portion of GO was dispersed in 35 mL ethanol by sonication for 30 min, forming stable graphene oxide colloid. Then 2.0 ml tetrabutyl titanate [Ti (O-Bu)<sub>4</sub>] was added with magnetic stirring for 15 min. The resulting suspension was transferred into a 50 ml Teflon-lined stainless steel autoclave and sealed tightly. The autoclave was then heated to 180 °C and kept there for 24 h. After the solvothermal treatment, the nanocomposite, was labeled as ATG<sub>ratio</sub> (e.g., ATG<sub>6.0</sub>, ATG<sub>2.4</sub> and ATG<sub>0.6</sub>) was then centrifuged, and washed with deionized water several times. The resulting products were dried in air at 60 °C overnight. For comparison, anatase TiO<sub>2</sub> was synthesized in the absence of GO via a similar procedure. Finally, heat treatment of TG<sub>6.0</sub> was done in air at different temperatures (200°C, 300°C and 400°C, respectively) for 3 h; the nanocomposite was labeled as ATG<sub>6.0-200</sub>, ATG<sub>6.0-300</sub> and ATG<sub>6.0-400</sub>.

### Characterization

Powder X-ray diffraction (XRD) analyses were performed on a Bruker D8 Advance diffractometer with Cu K $\alpha$  radiation ( $\lambda \approx 1.54 \text{ \AA}$ ). Fourier transform infrared (FTIR) spectra were carried out using a Shimadzu IR Prestige-21 spectrometer. Raman spectra were run on a Renishaw Raman microscope. Transmission electron microscopy (TEM) images were taken with a JEOL JEM-2100 transmission electron microscope.

### Photocatalytic Activity

The photocatalytic activities of the samples were evaluated by the decomposition of Reactive Black BL-G (RB BL-G) under UV irradiation using an XPA photochemical reactor (Nanjing Xujiang Factory of Electrical Engineering, Jiangsu, China). The irradiation was provided by a 500 W high-pressure mercury lamp with the main wave crest at 365 nm. The initial concentration of RB BL-G in a quartz reaction vessel was fixed at approximately 20mg·L<sup>-1</sup> with as-prepared catalysts loading of 0.2g·L<sup>-1</sup>. The solution was kept in the dark for 30 mins to reach an adsorption-desorption equilibrium with magnetic stirring. The reaction cell (450 mL) was bubbled with air at a flow rate of 40mL·min<sup>-1</sup>. At periodic intervals of time, the extent of RB BL-G decomposition was analyzed by recording variations of the absorption band maximum (595 nm) of RB BL-G using a BRAIC UV-1201 spectrophotometer.

## Results and Discussion

### Characterization of ATG Nanocomposites

The solvothermal method has been found to be a versatile method for the synthesis of a variety of TiO<sub>2</sub> nanoparticles with narrow size distribution and disparity<sup>[21]</sup> Furthermore, the graphene oxide could be reduced to graphene via solvothermal reaction as described previously<sup>[22]</sup> Figure 1 shows the XRD patterns of GO and ATG<sub>6.0</sub>, the spectral features of nanocomposites with other mass ratios are similar. The as-synthesized GO (Figure1a) shows a sharp peak at around  $2\theta = 10.5^\circ$ , corresponding to the (001) reflection of GO and the interlayer spacing (0.86 nm) was much larger than that of pristine graphite (0.34 nm) due to the introduction of oxygen-containing functional groups on the graphite sheets.<sup>[23]</sup> From Figure 1b, all the diffraction peaks of the ATG<sub>6.0</sub> can be indexed to synthesized anatase TiO<sub>2</sub> (JCPDS 21-1272, a=b=3.785Å, c=9.514 Å), and the (001) reflection peak of layered GO has almost disappeared, suggesting that the regular stacks of GO are exfoliated.<sup>[24]</sup>

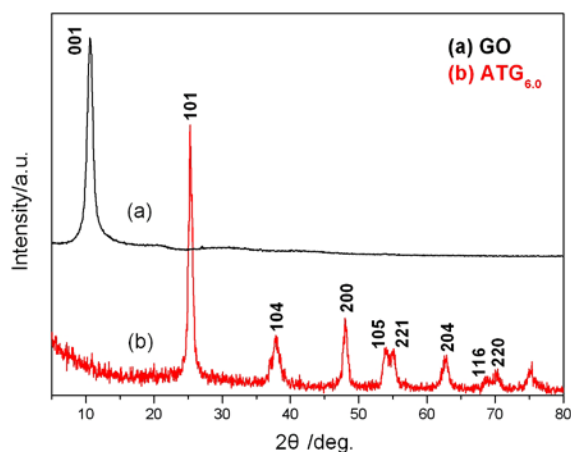


Figure 1 XRD patterns of samples (a) GO and (b) ATG<sub>6.0</sub>.

Figure 2a shows the FT-IR spectra of GO (curve 1) and ATG<sub>6.0</sub> (curve 2). The oxygen-containing functional groups of GO were revealed by the bands at 1051, 1223, 1402 and 1740 cm<sup>-1</sup> (curve 1), which correspond to C-O stretching vibrations, C-OH stretching peak, C-O-H deformation peak and C=O stretching of COOH groups, respectively. For ATG<sub>6.0</sub>, the absorption band appearing at around 1620 cm<sup>-1</sup> was attributed to the skeletal vibration of graphene sheets, and the bands related with the oxygen-containing functional groups almost disappeared (curve 2), indicating the graphene oxide had already been reduced to graphene during the solvothermal reaction. The broad absorption below 1000 cm<sup>-1</sup> showed the stretching vibration of Ti-O-Ti bonds. Furthermore, the increment of relative intensity of D/G in the Raman spectra of ATG<sub>6.0</sub> correlates well with the previous studies (Fig. 2b), indicating a decrease in the average size of the sp<sup>2</sup> domains but an increase in number upon deoxygenation.<sup>[25]</sup> The I<sub>D</sub>/I<sub>G</sub> ratio of ATG<sub>6.0</sub> is about 1.02, which is much higher than that of GO (0.68), indicative of the transformation of GO into rGO after solvothermal treatment. The Raman spectra of ATG<sub>6.0</sub> with small Raman shift (below 1000 cm<sup>-1</sup>) is displayed in the inset of Figure 2b, all of the peaks were assigned to the modes of anatase TiO<sub>2</sub>. A dominant peak centered at 146 cm<sup>-1</sup> was associated with E<sub>g</sub>(ν<sub>6</sub>) mode. Peaks centered at 395 and 510 cm<sup>-1</sup> were associated with B<sub>1g</sub> and A<sub>1g</sub> modes, and the 633 cm<sup>-1</sup> peak was assigned to E<sub>g</sub>(ν<sub>1</sub>). The FT-IR and Raman results indicate that graphene sheets and anatase TiO<sub>2</sub> coexist in the synthesized hybrids.

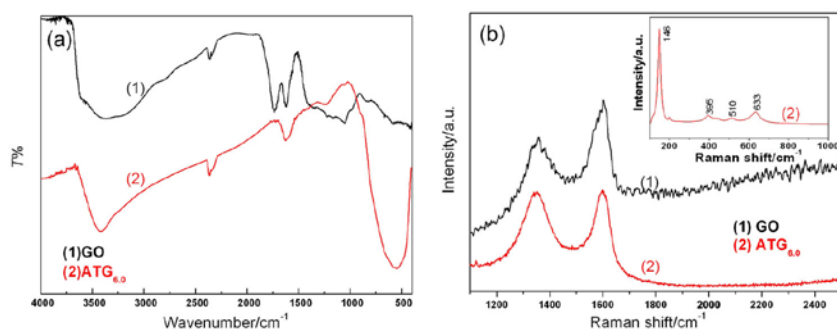


Figure 2 (a) FT-IR spectra of GO (1) and ATG<sub>6.0</sub> (2); (b) Raman spectra of GO (1) and ATG<sub>6.0</sub> (2)

The heterostructure of as-synthesized nanocomposites with different mass ratios of TiO<sub>2</sub>/GO were further examined using TEM. As showed in Figure 3, it is clearly seen from the panels a and b of Figure 3 that the almost transparent carbon sheets were decorated randomly by anatase TiO<sub>2</sub> nanoparticles with diameters ranging from 5 to 10 nm, and few particles broke away the carbon supports. Besides, anatase TiO<sub>2</sub> nanoparticles were inclined to accumulate along the wrinkles and edge, mainly due to the distribution of carboxylic acid groups at the edge of GO. With the increase of the mass ratio of TiO<sub>2</sub>/GO, the graphene sheets were coated by increased number of nanoparticles (Figure 3c-f). Fig. 3e and f display the highest density of anatase TiO<sub>2</sub> nanoparticles

on graphene sheets, which is essential to the photocatalytic activity of the composite.

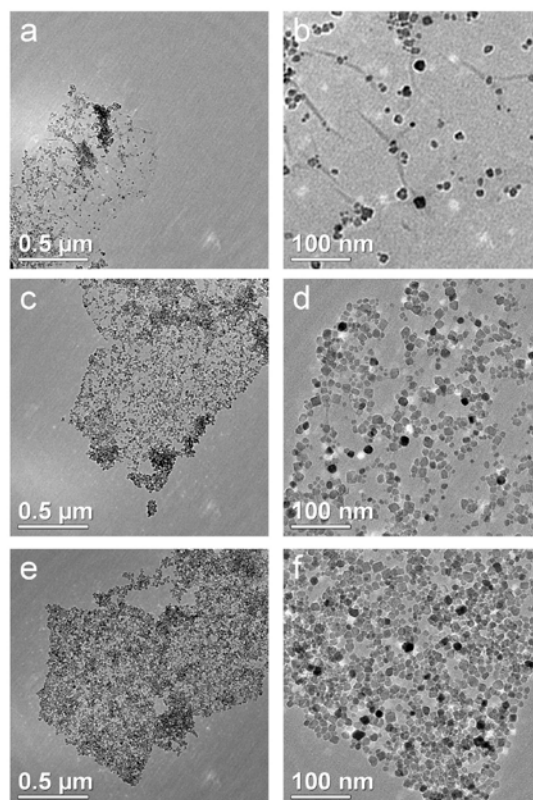


Figure 3 TEM images of (a, b) ATG6.0, (c, d) ATG2.4 and (e, f) ATG0.6

### Photocatalytic Properties of ATG Nanocomposites

The photocatalytic activities of a series of photocatalysts were measured by the degradation test of RB BL-G under UV irradiation, and the experimental results are shown in Figure 4 and Table 1. The normalized concentration of the solution ( $C/C_0$ ) is proportional to the normalized maximum absorbance ( $A/A_0$ ), therefore we can use  $C/C_0$  instead of  $A/A_0$ . It was clear that ATG composites had higher photocatalytic activity than the bare anatase  $\text{TiO}_2$ , mainly due to its two-dimensional planar structure, which is favorable for dye adsorption, charge transportation and UV rays reaching the anatase surface. With the increase of the mass ratios of  $\text{TiO}_2/\text{GO}$ , ATG nanocomposites showed significance progress in the photodegradation of RB BL-G. Figure 4b shows the photocatalytic activities of  $\text{ATG}_{6.0}$  after heat treatment at different temperature ( $200^\circ\text{C}$ ,  $300^\circ\text{C}$  and  $400^\circ\text{C}$ , respectively) for 3h. Although the absorption property of  $\text{ATG}_{6.0}$  was reduced with the increase of heat treatment temperature, the photocatalytic activity was enhanced gradually (see Table 1). Heat treatment of as-prepared photocatalysts at high temperature is beneficial to the crystallization of anatase  $\text{TiO}_2$ , which plays an important role in the photocatalytic reaction. Especially,  $\text{ATG}_{6.0-400}$  exhibited the highest photocatalytic activity that could degrade RB BL-G by 95.4% within 50 min (Table 1).

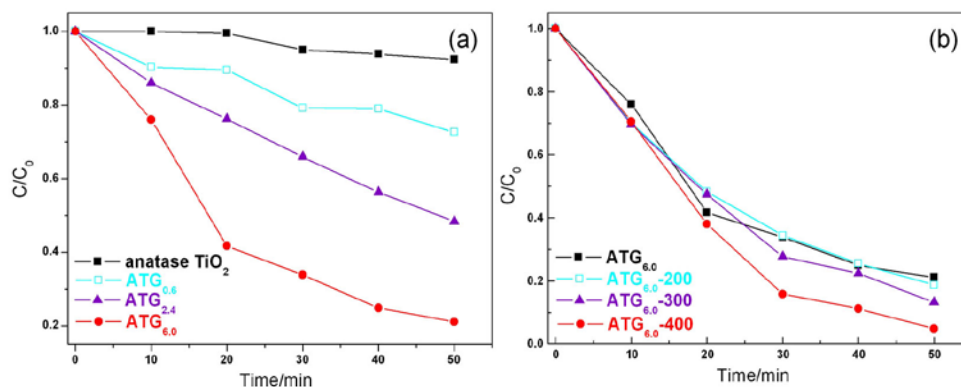


Figure 4 Photocatalytic degradation of RB BL-G by different different catalysts: (a) pure anatase  $TiO_2$  and ATG nanocomposites with different mass ratios of  $TiO_2/GO$ ; (b) ATG<sub>6.0</sub> before and after heat treatment at different temperatures.

Table 1 Absorption and photodecomposition rate of RB BL-G by different catalysts within 50 min.

Samples	anatase $TiO_2$	ATG <sub>0.6</sub>	ATG <sub>2.4</sub>	ATG <sub>6.0</sub>	ATG <sub>6.0</sub> -200	ATG <sub>6.0</sub> -300	ATG <sub>6.0</sub> -400
Absorption (%)	0	8.7	13.1	22.7	21.6	7.1	0.3
Removal rate of RB BL-G (%)	7.7	27.4	51.6	78.9	81.3	91.0	95.2

## Conclusions

In summary, ATG nanocomposites were successfully synthesized using a simple one-step solvothermal method. The characterization data for the nanocomposites indicated that the reduction of graphene oxide and loading of anatase  $TiO_2$  nanoparticles were achieved simultaneously. ATG photocatalyst exhibited much higher efficiency for the photodegradation of RB BL-G than mere anatase  $TiO_2$  due to its two-dimensional planar structure. Additionally, it was found that the photocatalytic activities of the nanocomposites were highly dependent upon the mass ratio of  $TiO_2/GO$ , and influenced markedly by heat treatment temperature.

## Acknowledgement

This work was supported by the Innovation Scientists and Technicians Troop Construction Projects of Henan Province (2013259), the Henan Province Key Discipline of Applied Chemistry (201218692) and Program for Innovative Research Team (in Science and Technology) in University of Henan Province (no. 14IRTSTHN009).

## References

- [1] Fujishima, A., Rao, T.N. & Tryk, D.A., Titanium dioxide photocatalysis. *J. Photochem. Photobiol. C*, 1(1), pp. 1-21, 2000.
- [2] Yang, J., Li, D., Wang, X., Yang, X. J. & Lu, L. D., Rapid synthesis of nanocrystalline  $TiO_2/SnO_2$  binary oxides and their photoinduced decomposition of methyl orange. *J. Solid. State. Chem.*, 165(1), pp. 193-198, 2002.

- [3] Zhang, L. L., Lv, F. J., Zhang, W. G., Li, R. Q., Zhong, H. & Zhao, Y. J., Photo degradation of methyl orange by attapulgite-SnO<sub>2</sub>-TiO<sub>2</sub> nanocomposites. *J. Hazard. Mater.*, 171(1), pp. 294-300, 2009.
- [4] Liu, H. J., Liu, G. G. & Zhou, Q. X., Preparation and characterization of Zr doped TiO<sub>2</sub> nanotube arrays on the titanium sheet and their enhanced photocatalytic activity. *J. Solid.State. Chem.*, 182(12), pp. 3238-3242, 2009.
- [5] Wang, D. & Astruc, D., Fast-growing field of magnetically recyclable nanocatalysts. *Chem. Rev.*, 114(14), pp. 6949-6985, 2014.
- [6] Zhang, G., Kima, G. & Choi, W., Visible light driven photocatalysis mediated via ligand-to-metal charge transfer (LMCT): an alternative approach to solar activation of titania. *Energy Environ.Sci.*, 7(3), pp. 954-966, 2014.
- [7] Moon, J., Takagi, H., Fujishiro, Y. & Awano, M., Preparation and characterization of the Sb-doped TiO<sub>2</sub> photocatalysts. *J. Mater.Sci.*, 36(4), pp. 949-955, 2001.
- [8] Ovenstone, J., Preparation of novel titania photocatalysts with high activity. *J. Mater. Sci.*, 36(6), pp. 1325-1329, 2001.
- [9] Woan, K., Pyrgiotakis, G. & Sigmund, W., Photocatalytic carbon-nanotube-TiO<sub>2</sub> composites. *Adv. Mater.* 21(21), pp.2233-2239, 2009.
- [10] Inagaki, M., Kojin, F., Tryba, B. & Toyoda, M., Carbon-coated anatase: the role of the carbon layer for photocatalytic performance. *Carbon*, 43(8), pp. 1652-1659, 2005.
- [11] Geim, A. K. & Novoselov, K.S., Detection of individual gas molecules adsorbed on graphene. *Nat. Mater.*, 6(9), pp. 183-191, 2007.
- [12] Li, D. & Kaner, R.B., Graphene-based materials. *Nat. Nanotechnol*, 3, pp. 101, 2008.
- [13] Stankovich, S., Dikin, D. A., Dommett, G. H. B., Kohlhaas, K. M., Zimney, E. J., Stach, E. A., Piner, R. D., Nguyen, S. T. & Ruoff, R. S., Graphene-based composite materials. *Nature*, 442(7100), pp. 282-286, 2006.
- [14] Yang, X., Qin, J., Li, Y., Zhang, R. & Huan, T., Graphene-spindle shaped TiO<sub>2</sub> mesocrystal composites: Facile synthesis and enhanced visible light photocatalytic performance. *J.hazard. Mater.* 261(15), pp. 342-350, 2013.
- [15] Wang, D. H., Choi, D. W., Li, J., Yang, Z. G., Nie, Z. M., Kou, R., Hu, D. H., Wang, C. M., Saraf, L. V., Zhang, J. G., Aksay, I. A. & Liu, J., Self-assembled TiO<sub>2</sub>-graphene hybrid nanostructures for enhanced Li-ion insertion. *ACS Nano*, 3(4), pp. 907-914, 2009.
- [16] Williams, G., Seger, B. & Kamat, P. V., TiO<sub>2</sub>-graphene nanocomposites, UV-assisted photocatalytic reduction of graphene oxide. *ACS Nano*, 2(7), pp. 1487-1491, 2008.
- [17] Zhang, X. Y., Li, H. P., Cui, X. L. & Lin, Y., Graphene/TiO<sub>2</sub> nanocomposites: synthesis, characterization and application in hydrogen evolution from water photocatalytic splitting. *J. Mater. Chem.*, 20(14), pp. 2801-2806, 2010.
- [18] Zhang, H., Lv, X. J., Li, Y. M. & Li, J. H., P25-graphene composite as a high performance photocatalyst. *ACS Nano*, 4(1), pp. 380-386, 2010.
- [19] Hummers, W. S. & Offeman, R. E., Preparation of graphitic oxide. *J. Am. Chem. Soc.*, 80(6), pp. 1339, 1958.
- [20] Kovtyukhova, N. I., Ollivier, P. J., Martin, B. R., Mallouk, T. E., Chizhik, S. A., Buzaneva, E. V. & Gorchinskiy, A. D., Layer-by-layer assembly of ultrathin composite films from micron-sized graphite oxide sheets and polycations. *Chem. Mater.*, 11(3), pp. 771-778, 1999.

- [21] Chen, X. B. & Mao, S. S., Titanium dioxide nanomaterials: synthesis, properties, modifications, and applications. *Chem. Rev.*, 107(7), pp. 2891-2959, 2007.
- [22] Nethravathi, C. & Rajamathi, M., Chemically modified graphene sheets produced by the solvothermal reduction of colloidal dispersions of graphite oxide. *Carbon*, 46(14), pp. 1994-1998, 2008.
- [23] Xu, C., Wu, X. D., Zhu, J. W. & Wang X., Synthesis of amphiphilic graphite oxide. *Carbon*, 46(2), pp. 386-389, 2007.
- [24] Xu, C., Wang, X. & Zhu, J. W., Graphene-metal particle nanocomposites. *J. Phys. Chem. C*, 112(50), pp. 19841-19845, 2008.
- [25] Stankovich, S., Dikin, D. A., Piner, R. D., Kohlhaas, K. A., Kleinhammes, A., Jia, Y. Y., Wu, Y., Nguyen, S. T. & Ruoff, R. S., Synthesis of graphene-based nanosheets via chemical reduction of exfoliated graphite oxide. *Carbon*, 45(7), pp. 1558-1565, 2007.